A NEW MIXED FINITE ELEMENT METHOD BASED ON THE CRANK-NICOLSON SCHEME FOR BURGERS' EQUATION

Xiaohui Hu, Pengzhan Huang, Xinlong Feng, Urumqi

Abstract. In this paper, a new mixed finite element method is used to approximate the solution as well as the flux of the 2D Burgers' equation. Based on this new formulation, we give the corresponding stable conforming finite element approximation for the $P_0^2 - P_1$ pair by using the Crank-Nicolson time-discretization scheme. Optimal error estimates are obtained. Finally, numerical experiments show the efficiency of the new mixed method and justify the theoretical results.

Keywords: Burgers' equation; mixed finite element method; stable conforming finite element; Crank-Nicolson scheme; inf-sup condition

MSC 2010: 65N30, 65N12, 65B05, 35Q30

1. Introduction

Burgers' equation was formulated by Bateman [2] in 1915, and can be regarded as a qualitative approximation of the Navier-Stokes equations. This equation incorporates both convection and diffusion, preserves the hybrid characteristic of the Navier-Stokes equations, and can be solved using similar numerical methods. As such, Burgers' equation is a good model for the numerical solution of the complicated Navier-Stokes equations. This equation is a hyperbolic-parabolic equation which has always been used as a mathematical model for many physical phenomena. It retains the nonlinear aspects of the governing equation in many practical transport problems such as aggregation interface growth, the formation of large-scale structures in the adhesion model for cosmology, turbulence transport, shock wave theory, wave

processes in thermoelastic medium, transport and dispersion of pollutants in rivers and sediment transport. Thus, the numerical method has practical significance, and has drawn the attention of many researchers. Burgers' equation is so important that many numerical methods for its solution were developed in the past decades. These methods include mainly the spectral method, the finite difference method, and the finite element method, see [3], [4], [5], [8], [9], [16], [18], [19], [21], and the references therein.

The mixed finite element method is frequently used to obtain approximate solutions to problems with more than one unknown. Accordingly, we need a finite element space for each unknown. These spaces must be chosen carefully so that they satisfy an inf-sup stability condition for the mixed method to be stable. Moreover, we can find the $P_0^2 - P_1$ finite element pair which satisfies the discrete inf-sup condition based on a new variational formulation of the two-dimensional Poisson equation [22] and the parabolic equation [23]. In fact, the issue considered in [23] is the linear problem, so we extend this new stable finite element method to solving Burgers' equation, which is a nonlinear PDE.

There exist several time-discretization methods to deal with Burgers' equation such as the backward Euler method, Crank-Nicolson method, Runge-Kutta method, etc. The Crank-Nicolson scheme [7] was first proposed by Crank and Nicolson for the heat-conduction equation in 1947, and it is unconditionally stable with second-order accuracy. Because of these properties, the scheme has been widely used in solving many PDEs [15], [23] and has drawn the attention of many researchers for Navier-Stokes equations [13], [12], [10], [17]. Hence, we use the Crank-Nicolson scheme and prove its optimal order of convergence.

This paper focuses on the Crank-Nicolson scheme for time discretization applied to the spatially discrete stable finite element approximation of Burgers' equation based on a lower regularity of the flux, and the nonlinear term is based on the Stokes iterative method [11]. Compared with the Newton iterative method and the Oseen iterative method, the Stokes iterative method takes less CPU time than the other two iterative methods, and has a better stability.

The outline of the paper is as follows. In Section 2, the basic notations and the new mixed formulation are stated. In Section 3, the stable mixed finite element pair $P_0^2 - P_1$ for Burgers' equation is shown. We discretize the given equation by the Crank-Nicolson mixed finite element method and derive optimal error estimates in Section 4. Results of the numerical experiments performed are discussed in Section 5, and the numerical experiments confirm the theoretical rate of convergence obtained. The conclusions are given in Section 6.

2. A NEW MIXED VARIATIONAL FORMULATION

In this paper, we consider the 2D Burgers' equation with homogeneous boundary condition:

$$u_t - \nu(u_{xx} + u_{yy}) + u(u_x + u_y) = f \quad \text{in } \Omega \times (0, T], \tag{2.1}$$

$$u(x, y, 0) = u_0(x, y) \quad \text{in } \Omega \times \{0\}, \tag{2.2}$$

$$u = 0 \quad \text{on } \partial\Omega \times (0, T], \tag{2.3}$$

where Ω is a bounded convex domain in the plane and $\partial\Omega$ is Lipschitz continuous boundary of Ω. The term $u_0(x, y)$ is the initial value, $T > 0$ represents the given final time, $f = f(x, y, t)$ is the prescribed force. The positive number $\nu = 1/\text{Re}$ is the coefficient of viscosity, and Re denotes the Reynolds number.

Suppose that $f \in L^2(\Omega)$. By introducing the flux $p = -\nabla u$, the mixed formulation of (2.1)–(2.3) is to find $(p, u) \in V \times W$ such that

$$(p, q) + (q, \nabla u) = 0 \quad \forall\, q \in V, \tag{2.4}$$

$$(u_t, v) - \nu(p, \nabla v) - ([u, u]p, v) = (f, v) \quad \forall\, v \in W. \tag{2.5}$$

Here we denote

$$V = L^2(\Omega)^2, \quad W = H_0^1(\Omega). \tag{2.6}$$

The Sobolev spaces used in this context are standard (see [1]). For example, for a bounded domain Ω, we denote by $H^m(\Omega)$ ($m \geqslant 0$) and $L^2(\Omega) = H^0(\Omega)$ the usual Sobolev spaces equipped with the seminorm and the norm, respectively,

$$|v|_{m,\Omega} = \left\{ \sum_{|\alpha|=m} \int_\Omega |D^\alpha v|^2 \, dx \, dy \right\}^{1/2} \quad \text{and} \quad \|v\|_{m,\Omega} = \left\{ \sum_{i=0}^m |v|_{i,\Omega}^2 \right\}^{1/2} \quad \forall\, v \in H^m(\Omega),$$

where $\alpha = (\alpha_1, \alpha_2)$, α_1 and α_2 are two nonnegative integers, and $|\alpha| = \alpha_1 + \alpha_2$. Especially, the subspace $H_0^1(\Omega)$ of $H^1(\Omega)$ is denoted by $H_0^1(\Omega) = \{v \in H^1(\Omega); v|_{\partial\Omega} = 0\}$. Note that $\|\cdot\|_1$ is equivalent to $|\cdot|_1$ in $H_0^1(\Omega)$.

For any $t \in [0, T]$, we define the following bilinear forms:

$$a(p, q) = (p, q) \quad \forall\, p, q \in V, \tag{2.7}$$

$$b(p, v) = -(p, \nabla v) \quad \forall\, p \in V, \quad \forall\, v \in W. \tag{2.8}$$

From (2.4)–(2.5), for any $t \in [0, T]$, a new variational formulation to Burgers' equation (2.1)–(2.3) is to find $(p, u) \in V \times W$ such that

$$(2.9) \qquad\qquad a(p, q) - b(q, u) = 0 \quad \forall q \in V,$$

$$(2.10) \qquad (u_t, v) + \nu b(p, v) - ([u, u]p, v) = (f, v) \quad \forall v \in W.$$

Obviously, (2.9)–(2.10) is a saddle point system. Concerning this system, we give some properties in the following two lemmas.

Lemma 2.1 ([22]). *The bilinear form $b(\cdot, \cdot)$ given by (2.8) satisfies the so-called inf-sup condition, i.e., there exists a constant $\beta_1 > 0$ such that*

$$(2.11) \qquad\qquad \inf_{v \in W} \sup_{q \in V} \frac{-(q, \nabla v)}{\|q\|_V \|v\|_W} \geqslant \beta_1.$$

Throughout the paper, C indicates a positive constant which is possibly different at different occurrences, being independent of the spatial and time mesh sizes, but may depend on Ω, the Reynolds number, and other parameters introduced in this paper.

Lemma 2.2 ([6]). *Let $g(t)$ be integrable on $[0, T]$ and almost everywhere positive function. If $\psi(t) \in C^0([0, T])$ satisfies the inequality*

$$0 \leqslant \psi(t) \leqslant C + \int_0^t g(s)\psi(s)\, \mathrm{d}s \quad \forall t \in [0, T],$$

then $\psi(t)$ also satisfies

$$0 \leqslant \psi(t) \leqslant C \exp\left(\int_0^t g(s)\, \mathrm{d}s \right) \quad \forall t \in [0, T].$$

Furthermore, if $C = 0$ then $\psi(t) \equiv 0$.

Theorem 2.3. *Suppose that $u_0(x, y) \in L^2(\Omega)$. Then there exists a unique solution $(p, u) \in V \times W$ to variational formulation (2.9)–(2.10). Moreover, there exists a constant $M_0 > 0$ such that $\|u\|_{0,\infty} \leqslant M_0$.*

P r o o f. From [20], we know that there exists a unique solution u to (2.1)–(2.3). Hence, $(p, u) = (-\nabla u, u)$ is a solution of variational formulation (2.9)–(2.10). From the sum of (2.9) with $q = \nabla u$ and (2.10) with $v = u$, applying $([u, u]p, u) = 0$, we obtain

$$\frac{1}{2} \frac{\mathrm{d}}{\mathrm{d}t} \|u\|_0^2 + \nu \|\nabla u\|_0^2 = (f, u).$$

Integrating the above equation from 0 to t and applying the initial condition, we get

$$(2.12) \qquad \|u\|_0^2 + 2\nu \int_0^t \|\nabla u\|_0^2 \, \mathrm{d}s = \|u_0\|_0^2 + 2 \int_0^t (f, u) \, \mathrm{d}s.$$

By the boundedness of the integration and using (2.12), there exists a constant C_0 such that

$$(2.13) \qquad \|\nabla u\|_0 \leqslant C_0.$$

And by the embedding theorem of Sobolev space (see [1], [6]), there exists a constant C_1 such that

$$(2.14) \qquad \|u\|_{0,\infty} \leqslant C_1 \|\nabla u\|_0 \leqslant C_1 C_0 \equiv M_0.$$

Let (p^*, u^*) be another solution to (2.9)–(2.10). Then $\|u^*\|_{0,\infty} \leqslant M_0$. And combining (2.9) with (2.10), we derive

$$(2.15) \qquad (p - p^*, q) + (q, \nabla(u - u^*)) = 0 \quad \forall q \in V,$$
$$(2.16) \quad (u_t - u_t^*, v) - \nu(p - p^*, \nabla v) - ([u, u]p - [u^*, u^*]p^*, v) = 0 \quad \forall v \in W.$$

From the sum of (2.15) with $q = p - p^*$ and (2.16) with $v = u - u^*$, applying the Cauchy-Schwarz and Young inequalities, we have

$$(2.17) \quad \frac{1}{2} \frac{\mathrm{d}}{\mathrm{d}t} \|u - u^*\|_0^2 + \nu \|p - p^*\|_0^2 = ([u, u]p - [u^*, u^*]p^*, u - u^*)$$
$$\leqslant M_0 \|p - p^*\|_0 \|u - u^*\|_0 + M_0 \|u - u^*\|_0^2$$
$$\leqslant \frac{M_0^2}{2} \|p - p^*\|_0^2 + \frac{1}{2} \|u - u^*\|_0^2 + M_0 \|u - u^*\|_0^2$$
$$= \frac{M_0^2}{2} \|p - p^*\|_0^2 + \left(\frac{1}{2} + M_0 \right) \|u - u^*\|_0^2.$$

By a simple computation, we have

$$(2.18) \qquad \frac{1}{2\nu - M_0^2} \frac{\mathrm{d}}{\mathrm{d}t} \|u - u^*\|_0^2 + \|p - p^*\|_0^2 \leqslant \frac{1 + 2M_0}{2\nu - M_0^2} \|u - u^*\|_0^2.$$

Integrating (2.18) from 0 to t and noting that $(u - u^*)(0) = 0$, we get

$$(2.19) \qquad \|u - u^*\|_0^2 \leqslant (1 + 2M_0) \int_0^t \|u - u^*\|_0^2 \, \mathrm{d}s \quad \forall t \in [0, T].$$

By Lemma 2.2, $\|u - u^*\|_0 = 0$, i.e., $u = u^*$. Consequently, by (2.18), $\|p - p^*\|_0 = 0$, i.e., $p = p^*$. The proof is completed. $\qquad \square$

3. Finite element approximation

In this section, based on the new variational formulation (2.9)–(2.10), we address the stable conforming finite element approximation for the $P_0^2 - P_1$ pair. Let K_h be a uniformly regular family of triangulations of $\overline{\Omega}$. Now, choose (V_h, W_h) as the $P_0^2 - P_1$ finite element pair as follows:

$$(3.1) \qquad V_h = \{q_h = (q_1, q_2) \in V \colon q_i \in P_0(T) \; \forall T \in K_h, \; i = 1, 2\},$$

$$(3.2) \qquad W_h = \{v \in C^0(\Omega) \cap W \colon v \in P_1(T) \; \forall T \in K_h\}.$$

Lemma 3.1. ([22]). *The $P_0^2 - P_1$ finite element pair defined by the spaces (3.1) and (3.2) satisfies the discrete inf-sup condition as follows:*

$$(3.3) \qquad \inf_{v_h \in W_h} \sup_{q_h \in V_h} \frac{-(q_h, \nabla v_h)}{\|q_h\|_V \|v_h\|_W} \geqslant \beta_2 > 0.$$

Lemma 3.2 ([23]). *There exists a standard L^2-projection operator $\Pi \colon L^2(\Omega) \to V_h$ which satisfies the following properties:*

$$(3.4) \qquad (p - \Pi p, q) = 0 \quad \forall q \in V_h,$$

$$(3.5) \qquad \|\Pi p\|_0 \leqslant C\|p\|_0 \quad \forall p \in V,$$

$$(3.6) \qquad \|p - \Pi p\|_0 \leqslant Ch\|p\|_1 \quad \forall p \in H^1(\Omega) \cap V.$$

Lemma 3.3 ([23]). *There exists a projection $\Lambda \colon W \to W_h$ such that*

$$(3.7) \qquad \|\Lambda u\|_0 \leqslant C\|u\|_1 \quad \forall u \in W,$$

$$(3.8) \qquad \|u - \Lambda u\|_0 + h\|u - \Lambda u\|_1 \leqslant Ch^2\|u\|_2 \quad \forall u \in H^2(\Omega) \cap W,$$

and if $u \in H_0^1(\Omega)$, then we have

$$(3.9) \qquad (\nabla(u - \Lambda u), q) = 0 \quad \forall q \in V_h.$$

By using a similar argument as in [18], we have the following result.

Theorem 3.4. *If $u_0(x, y) \in L^2(\Omega)$, then there exists a unique finite element solution $(p_h, u_h) \in V_h \times W_h$ to the following equations for $P_0^2 - P_1$ finite element pair:*

$$(3.10) \qquad a(p_h, q) - b(q, u_h) = 0 \quad \forall\, q \in V_h,$$

$$(3.11) \qquad (u_{ht}, v) + \nu b(p_h, v) - ([u_h, u_h]p_h, v) = (f, v) \quad \forall\, v \in W_h.$$

Moreover, there exists a constant M_1 independent of h such that

$$(3.12) \qquad \|u_h\|_0 \leqslant M_1.$$

4. Mixed finite element approximation based on the Crank-Nicolson scheme

Let $\tau = T/N$ be the time step and u_h^n be the approximation of $u(t)$ at $t = t_n = n\tau$ $(n = 1, 2, \ldots, N)$ in W_h. Applying the Crank-Nicolson scheme to the time derivative $\partial u/\partial t$ around the point $t_{n-1/2} = (n - 1/2)\tau$, we obtain the following fully discrete formulation:

$$(4.1) \left(\frac{u_h^n - u_h^{n-1}}{\tau}, v\right) - \nu\left(\frac{p_h^n + p_h^{n-1}}{2}, \nabla v\right) - \left(\frac{\psi_h^n + \psi_h^{n-1}}{2}, v\right) = \left(\frac{f^n + f^{n-1}}{2}, v\right),$$

$$(4.2) \qquad \left(\frac{p_h^n + p_h^{n-1}}{2}, q\right) + \left(q, \nabla\frac{u_h^n + u_h^{n-1}}{2}\right) = 0,$$

$$(4.3) \qquad (u_h^0, v) = (\Lambda u^0, v),$$

$$(4.4) \qquad (p_h^0, q) + (\nabla\Lambda u^0, q) = 0,$$

where $\psi_h^n = [u_h^n, u_h^n]p_h^n$, $v \in W_h$, $q \in V_h$.

Set $\varepsilon^n = u^n - u_h^n$ and $\eta^n = p^n - p_h^n$. Using (4.1) and (4.2) for any $q \in V_h$ and $v \in W_h$, we obtain the error equations as follows:

$$(4.5) \quad \left(\frac{\varepsilon^n - \varepsilon^{n-1}}{\tau}, v\right) - \nu\left(\frac{\eta^n + \eta^{n-1}}{2}, \nabla v\right) - \left(\frac{\varphi_h^n}{2}, v\right) - \left(\frac{\varphi_h^{n-1}}{2}, v\right)$$
$$= \left(\frac{u^n - u^{n-1}}{\tau} - u_t^{n-1/2}, v\right) - \left(\frac{u_t^n + u_t^{n-1}}{2} - u_t^{n-1/2}, v\right),$$

$$(4.6) \quad \left(\frac{\eta^n + \eta^{n-1}}{2}, q\right) + \left(q, \nabla\frac{\varepsilon^n + \varepsilon^{n-1}}{2}\right) = 0.$$

Here, $\varphi_h^n = [u^n, u^n]p^n - [u_h^n, u_h^n]p_h^n$, $(u^n - u^{n-1})/\tau - u_t^{n-1/2}$ is the truncation error associated with the Crank-Nicolson method to the time derivative.

In order to obtain the error estimate, we introduce some useful lemmas as follows:

Lemma 4.1 ([6])**.** *Let C and a_k, c_k, d_k for integer $k \geqslant 0$ be nonnegative numbers such that*

$$a_n \leqslant \tau \sum_{k=0}^{n-1} d_k a_k + \tau \sum_{k=0}^{n-1} c_k + C \quad \forall\, n \geqslant 1.$$

Then

$$a_n \leqslant \exp\left(\tau \sum_{k=0}^{n-1} d_k \right) \left(\tau \sum_{k=0}^{n-1} c_k + C \right) \quad \forall\, n \geqslant 1.$$

Lemma 4.2 ([23])**.** *For each $n \geqslant 1$, if $u_{tt}, u_{ttt} \in L^2(0, T; L^2(\Omega))$, then we have*

$$\left\| \frac{u^n + u^{n-1}}{2} - u^{n-1/2} \right\|^2 \leqslant C\tau^3 \int_{t_{n-1}}^{t_n} \|u_{tt}\|^2 \, \mathrm{d}t,$$

$$\left\| \frac{u^n - u^{n-1}}{\tau} - u_t^{n-1/2} \right\|^2 \leqslant C\tau^3 \int_{t_{n-1}}^{t_n} \|u_{ttt}\|^2 \, \mathrm{d}t.$$

Theorem 4.3. *For the $P_0^2 - P_1$ finite element pair there exists a positive constant C such that*

(4.7)

$$\|u^n - u_h^n\|_1 + \|p^n - p_h^n\|_0 \leqslant Ch\left(\|u^0\|_2 + \|p^0\|_1 + \int_0^{t_n} \|u_t\|_2 \, \mathrm{d}t + \int_0^{t_n} \|p_t\|_1 \, \mathrm{d}t \right)$$

$$+ C\tau^2 \left(\int_0^{t_n} \|u_{ttt}\|_0^2 \, \mathrm{d}t \right)^{1/2}.$$

Furthermore, we have

(4.8) $\qquad \|u^n - u_h^n\|_0 \leqslant Ch^2\left(\|u^0\|_2 + \int_0^{t_n} \|u_t\|_2 \, \mathrm{d}t \right) + C\tau^2 \left(\int_0^{t_n} \|u_{ttt}\|_0^2 \, \mathrm{d}t \right)^{1/2}.$

P r o o f. Let

$$u^n - u_h^n = u^n - \Lambda u^n + \Lambda u^n - u_h^n = \varphi^n + \theta^n = \varepsilon^n,$$
$$p^n - p_h^n = p^n - \Pi p^n + \Pi p^n - p_h^n = \varrho^n + \xi^n = \eta^n.$$

From (3.6) and (3.8), we have

(4.9) $\qquad \|\varphi^n\|_1 = \|u^n - \Lambda u^n\|_1 \leqslant Ch\left(\|u^0\|_2 + \int_0^{t_n} \|u_t\|_2 \, \mathrm{d}t \right),$

(4.10) $\qquad \|\varphi^n\|_0 = \|u^n - \Lambda u^n\|_0 \leqslant Ch^2\left(\|u^0\|_2 + \int_0^{t_n} \|u_t\|_2 \, \mathrm{d}t \right),$

(4.11) $\qquad \|\varrho^n\|_0 = \|p^n - \Pi p^n\|_0 \leqslant Ch\left(\|p^0\|_1 + \int_0^{t_n} \|p_t\|_1 \, \mathrm{d}t \right).$

34

And for any $v \in W_h$ and $q \in V_h$, from (3.4) and (3.9), we get

$$(4.12) \quad \left(\frac{\theta^n - \theta^{n-1}}{\tau}, v \right) - \nu \left(\frac{\xi^n + \xi^{n-1}}{2}, \nabla v \right) - \left(\frac{\varphi_h^n}{2}, v \right) - \left(\frac{\varphi_h^{n-1}}{2}, v \right)$$

$$= \left(\frac{u^n - u^{n-1}}{\tau} - u_t^{n-1/2}, v \right) - \left(\frac{u_t^n + u_t^{n-1}}{2} - u_t^{n-1/2}, v \right),$$

$$(4.13) \quad \left(\frac{\xi^n + \xi^{n-1}}{2}, q \right) + \left(q, \nabla \frac{\theta^n + \theta^{n-1}}{2} \right) = 0.$$

We consider

$$(4.14) \qquad \left(\frac{\xi^n - \xi^{n-1}}{\tau}, q \right) + \left(q, \nabla \frac{\theta^n - \theta^{n-1}}{\tau} \right) = 0 \quad \forall q \in V_h, \ n = 1, 2, \ldots, N,$$

instead of (4.13). From (4.13) and taking $q = \nabla(\theta^n - \theta^{n-1})/2$, applying the Cauchy-Schwarz and Young inequalities, we obtain

$$\|\nabla \theta^n\|_0^2 - \|\nabla \theta^{n-1}\|_0^2 \leqslant \|\xi^n + \xi^{n-1}\|_0 \|\nabla \theta^n + \nabla \theta^{n-1}\|_0$$

$$\leqslant \frac{\|\xi^n + \xi^{n-1}\|_0^2}{2\delta} + \frac{\delta \|\nabla \theta^n + \nabla \theta^{n-1}\|_0^2}{2}.$$

Choosing $\delta \geqslant 0$ such that $1 - \delta > 0$ and due to Poincaré inequality, we have

$$\|\theta^n\|_1^2 \leqslant C(\|\theta^{n-1}\|_1^2 + \|\xi^n\|_0^2).$$

Considering $u_h^0 = \Lambda u^0$ and adding all equations for each n with $1 \leqslant n \leqslant N$ from Lemma 4.1, we get

$$(4.15) \qquad\qquad\qquad\qquad \|\theta^n\|_1 \leqslant C_1 \|\xi^n\|_0.$$

From the sum of (4.12) with $v = (\theta^n - \theta^{n-1})/\tau$ and (4.14) with $q = (\xi^n + \xi^{n-1})/2$, applying the Cauchy-Schwarz and Young inequalities and Lemma 4.2, we obtain

$$(4.16) \qquad \nu(\|\xi^n\|_0^2 - \|\xi^{n-1}\|_0^2) \leqslant (\varphi_h^{n-1}, \theta^n - \theta^{n-1}) + (\varphi_h^n, \theta^n - \theta^{n-1})$$

$$+ C\tau^4 \int_{t_{n-1}}^{t_n} \|u_{ttt}\|_0^2 \, \mathrm{d}t.$$

From Theorem 2.3 and Theorem 3.4, using (4.10), (4.11), (4.15), and applying the Cauchy-Schwarz and Young inequalities again, we obtain

$$
\begin{aligned}
(4.17)\quad & (\varphi_h^{n-1}, \theta^n - \theta^{n-1}) \\
&= ([u^{n-1}, u^{n-1}](\varrho^{n-1} + \xi^{n-1}) + p_h^{n-1}[\varphi^{n-1} + \theta^{n-1}, \varphi^{n-1} + \theta^{n-1}], \theta^n - \theta^{n-1}) \\
&\leqslant \frac{\delta_1 M_0^2}{2} \|\varrho^{n-1} + \xi^{n-1}\|^2 + \frac{\delta_2 M_1^2}{2} \|\varphi^{n-1} + \theta^{n-1}\|^2 + \Big(\frac{1}{2\delta_1} + \frac{1}{2\delta_2}\Big) \|\theta^n - \theta^{n-1}\|^2 \\
&\leqslant Ch^2 \bigg[\Big(\|p^0\|_1 + \int_0^{t_{n-1}} \|p_t\|_1 \, \mathrm{d}t\Big)^2 + \Big(\|u^0\|_2 + \int_0^{t_{n-1}} \|u_t\|_2 \, \mathrm{d}t\Big)^2\bigg] + C\|\xi^{n-1}\|^2 \\
&\quad + \Big(\frac{1}{2\delta_1} + \frac{1}{2\delta_2}\Big)\Big(1 + \frac{1}{\delta_3}\Big) C_1 \|\xi^n\|^2.
\end{aligned}
$$

The second term of the right-hand side of (4.16) is similar to (4.17). Here the constants of the Young inequality are chosen appropriately such that the coefficient of $\|\xi^n\|^2$ in the right-hand side of (4.16) is less than ν. Combining (4.16) with (4.17), adding all equations for each n with $1 \leqslant n \leqslant N$, from Lemma 4.1, we have

$$
\begin{aligned}
(4.18)\quad \|\xi^n\|_0 \leqslant{}& Ch\bigg(\|u^0\|_2 + \|p^0\|_1 + \int_0^{t_n} \|u_t\|_2 \, \mathrm{d}t + \int_0^{t_n} \|p_t\|_1 \, \mathrm{d}t\bigg) \\
&+ C\tau^2 \bigg(\int_0^{t_n} \|u_{ttt}\|_0^2 \, \mathrm{d}t\bigg)^{1/2}.
\end{aligned}
$$

Consequently, using (4.9), (4.11), (4.15), (4.18) and the triangle inequality, we complete the proof of (4.7).

Moreover, we need to prove (4.8). Taking $v = (\theta^n - \theta^{n-1})/\tau$, $q = \nabla(\theta^n - \theta^{n-1})/\tau$, applying the Cauchy-Schwarz and Young inequalities, we obtain from the sum of (4.12) and (4.13) that

$$
\begin{aligned}
(4.19)\quad \nu(\|\nabla\theta^n\|_0^2 - \|\nabla\theta^{n-1}\|_0^2) \leqslant{}& (\varphi_h^{n-1}, \theta^n - \theta^{n-1}) + (\varphi_h^n, \theta^n - \theta^{n-1}) \\
&+ C\tau^4 \int_{t_{n-1}}^{t_n} \|u_{ttt}\|_0^2 \, \mathrm{d}t.
\end{aligned}
$$

From Theorem 2.3 and Theorem 3.4, using Green's formula, applying the Cauchy-Schwarz and Young inequalities, we obtain

$$
\begin{aligned}
(4.20)\quad & (\varphi_h^{n-1}, \theta^n - \theta^{n-1}) \\
&= ([u_h^{n-1}, u_h^{n-1}]\nabla u_h^{n-1}, \theta^n - \theta^{n-1}) - ([u^{n-1}, u^{n-1}]\nabla u^{n-1}, \theta^n - \theta^{n-1}) \\
&= ([(u^{n-1})^2 - (u_h^{n-1})^2, (u^{n-1})^2 - (u_h^{n-1})^2], \nabla(\theta^n - \theta^{n-1})) \\
&\leqslant C\|\varphi^{n-1}\|_0^2 + C\|\nabla\theta^{n-1}\|_0^2 + \frac{1}{2\varepsilon_1}\Big(1 + \frac{1}{\varepsilon_2}\Big)\|\nabla\theta^n\|_0^2.
\end{aligned}
$$

Similarly,

$$(4.21) \quad (\varphi_h^n, \theta^n - \theta^{n-1}) = ([u_h^n, u_h^n] \nabla u_h^n, \theta^n - \theta^{n-1}) - ([u^n, u^n] \nabla u^n, \theta^n - \theta^{n-1})$$

$$\leqslant \left[\frac{\varepsilon_3}{4}(M_0 + M_1)^2 (1 + \varepsilon_4) + \frac{1}{2\varepsilon_3}(1 + \varepsilon_5) \right] \|\nabla \theta^n\|_0^2$$

$$+ C\|\varphi^n\|_0^2 + C\|\nabla \theta^{n-1}\|_0^2.$$

Here ε_i $(i = 1, 2, \ldots, 5)$ are chosen appropriately such that the coefficient of $\|\nabla \theta^n\|_0^2$ in the right-hand side of (4.19) is less than ν. Combining (4.19)–(4.21), using (4.10), adding all equations for each n with $1 \leqslant n \leqslant N$, from Lemma 4.1, we have

$$(4.22) \qquad \|\theta^n\|_0 \leqslant Ch^2 \left(\|u^0\|_2 + \int_0^{t_n} \|u_t\|_2 \, \mathrm{d}t \right) + C\tau^2 \left(\int_0^{t_n} \|u_{ttt}\|_0^2 \, \mathrm{d}t \right)^{1/2}.$$

Consequently, using (4.10), (4.22), and the triangle inequality, we complete the proof of (4.8). $\qquad\square$

5. Numerical experiments

In this section, we report three numerical examples for Burgers' equation with the new mixed finite element method based on the Crank-Nicolson scheme. In the first example, the accuracy and the convergence rate of our method are checked, and the results are obtained and compared by using the Stokes, Newton, and Oseen iteration method [11] to nonlinear term, respectively. In the second example, we take numerical solutions computed on a very fine mesh as the "exact" solutions, and compare the numerical solutions with them. In the third example, for Burgers' equation with mixed initial boundary value problems, we simulate the numerical solutions for the velocity and flux. Our algorithms are implemented using the public domain finite element software [14].

E x a m p l e 1. The exact solution u is given as follows:

$$u = (t + 1)x^2(x - 1)y(y - 1).$$

The initial condition in (2.2) is set according to the exact solution and the right-hand side $f(x, y, t)$ determined by (2.1). Here, the final time $T = 1$. In this experiment, Ω is the unit square $[0, 1] \times [0, 1]$ in $\mathbb{R}^2$. The mesh is obtained by dividing Ω into squares and then drawing a diagonal in each square.

In Tables 1–3, we show the convergence of the three methods when we take $\tau = h$ for the $P_0^2 - P_1$ finite element pair based on the Crank-Nicolson scheme in time. We obtain the optimal error estimates in Theorem 4.3. Obviously, we get the same performance in convergence aspect in these tables for the three schemes. And the three schemes keep the convergence rates just like the theoretical analysis. We also give the CPU time of these three schemes in Tables 1–3. From the three tables, we know that computing Burgers' equation by using the Stokes scheme takes less CPU time than the other two schemes, and the Newton scheme takes the most time. In the experiment, for $\nu = 1$, $\tau = h = 1/64$, the computing time of the Stokes scheme, Oseen scheme, and Newton scheme are 90.89 s, 93.547 s, 102.906 s, respectively.

$1/h$	$\dfrac{\|u - u_h\|_0}{\|u\|_0}$	u_{L^2}-rate	$\dfrac{\|u - u_h\|_1}{\|u\|_1}$	u_{H^1}-rate	$\dfrac{\|p - p_h\|_0}{\|p\|_0}$	p_{L^2}-rate	CPU time
4	0.207764	—	0.465188	—	0.368905	—	0.031 s
8	0.057550	1.8521	0.241289	0.9470	0.190730	0.9517	0.187 s
16	0.014733	1.9658	0.121768	0.9866	0.096134	0.9884	1.406 s
32	0.003705	1.9914	0.061026	0.9966	0.048163	0.9971	11.437 s
64	0.000928	1.9975	0.030531	0.9992	0.024093	0.9993	90.890 s

Table 1. Relative error and convergence rate of the Stokes scheme for the velocity and flux with $\tau = h$.

$1/h$	$\dfrac{\|u - u_h\|_0}{\|u\|_0}$	u_{L^2}-rate	$\dfrac{\|u - u_h\|_1}{\|u\|_1}$	u_{H^1}-rate	$\dfrac{\|p - p_h\|_0}{\|p\|_0}$	p_{L^2}-rate	CPU time
4	0.208259	—	0.465212	—	0.368928	—	0.031 s
8	0.057627	1.8536	0.241287	0.9471	0.190722	0.9519	0.203 s
16	0.014742	1.9668	0.121767	0.9866	0.096132	0.9884	1.609 s
32	0.003706	1.9920	0.061026	0.9966	0.048162	0.9971	12.969 s
64	0.000928	1.9978	0.030531	0.9992	0.024093	0.9993	102.906 s

Table 2. Relative error and convergence rate of the Newton scheme for the velocity and flux with $\tau = h$.

$1/h$	$\dfrac{\|u - u_h\|_0}{\|u\|_0}$	u_{L^2}-rate	$\dfrac{\|u - u_h\|_1}{\|u\|_1}$	u_{H^1}-rate	$\dfrac{\|p - p_h\|_0}{\|p\|_0}$	p_{L^2}-rate	CPU time
4	0.208387	—	0.465217	—	0.368944	—	0.031 s
8	0.057632	1.8543	0.241288	0.9471	0.190726	0.9519	0.187 s
16	0.014742	1.9669	0.121767	0.9866	0.096133	0.9884	1.453 s
32	0.003706	1.9920	0.061026	0.9966	0.048163	0.9971	11.703 s
64	0.000928	1.9981	0.030531	0.9992	0.024093	0.9993	93.547 s

Table 3. Relative error and convergence rate of the Oseen scheme for the velocity and flux with $\tau = h$.

Moreover, according to the numerical results given in Tables 1–3, the velocity for the L^2-norm error convergence order, the H^1-norm error convergence order, and the flux for the L^2-norm error convergence order are shown in Fig. 1. From the three plots, we can see that the convergence orders of the three schemes are substantially coincident, and this shows that the results are reasonable.
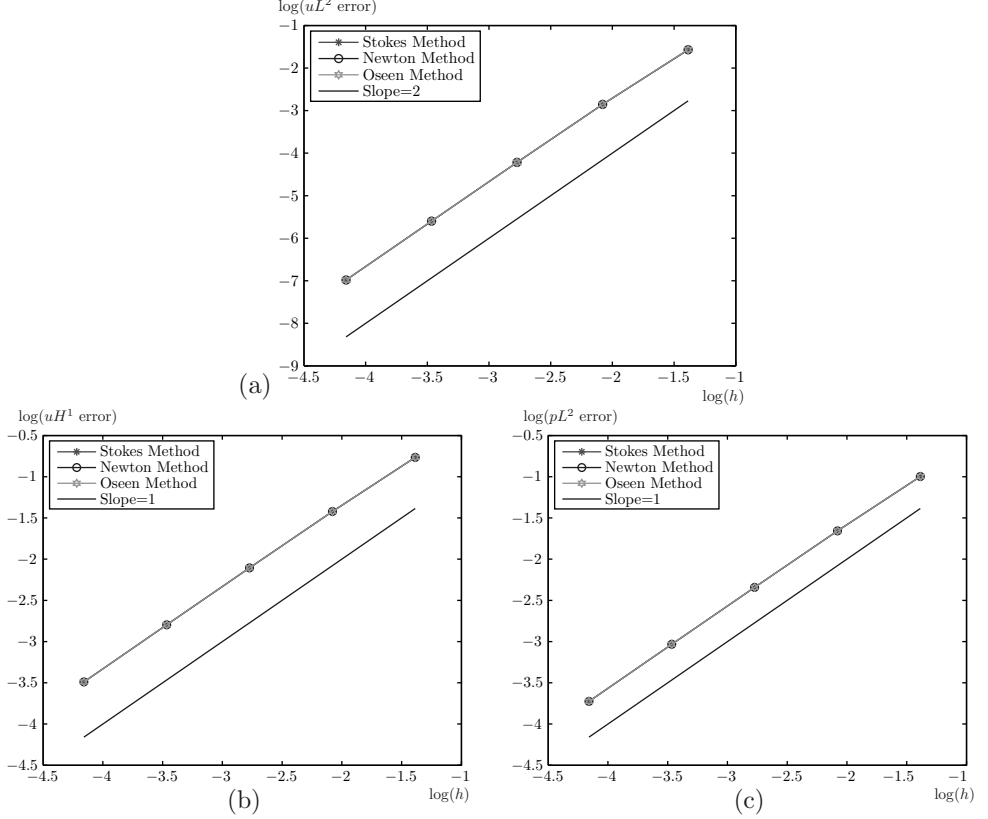

Figure 1. Three schemes on the velocity and flux of the error convergence order for $\nu = 1$: (a) the velocity for the L^2-error convergence order, (b) the velocity for the H^1-error convergence order, (c) the flux for the L^2-error convergence order.

E x a m p l e 2. In this example, we consider Burgers' equation (2.1) in $(x, y) \in [0, 1] \times [0, 1]$ with $f = 0$, which satisfies periodic boundary condition, and the corresponding initial value is

$$u(x, y, 0) = \sin(2\pi x)\cos(2\pi y).$$

As can be seen from the above example, the Stokes iteration method takes the least time, so we compute the solutions using the Stokes scheme at $t = 1/8$, where

the viscosity $\nu = 0.01$. The exact solution of this problem is unknown. Thus, we take the numerical solution by the standard Galerkin method (the Taylor-Hood element) computed on a very fine mesh (4225 grid points) as the "exact" solution for the purpose of comparison. The $x - y$ solution contours are plotted in Fig. 2 for numerical solution with grid points $N = 1089$, and the "exact" solution. We can see that the numerical solution agrees well with the "exact" solution.
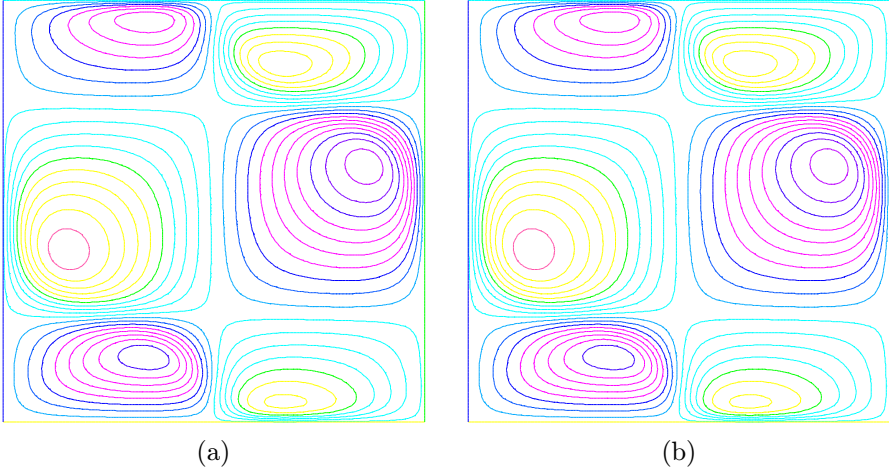

(a)　　　　　　　　　　　　(b)

Figure 2. $x - y$ solution contours for $\nu = 0.01$: (a) numerical solution, (b) "exact" solution.

E x a m p l e 3. Here we consider Burgers' equation (2.1) in L-shape with $f = 0$, which satisfies the following mixed boundary conditions

$$u = \frac{1}{1 + \exp((x + y - t)/2\nu)} \quad \text{on } \Gamma_D, \quad \frac{\partial u}{\partial n} = 0 \quad \text{on } \Gamma_N,$$

and the initial condition

$$u(x, y, 0) = \frac{1}{1 + \exp((x + y)/2\nu)},$$

where $\Gamma_N = \{(x, y); \ 0 \leqslant x \leqslant 1, \ y = 0\} \cup \{(x, y); \ x = 0, 0 \leqslant y \leqslant 1\}$, $\Gamma_D = \partial\Omega \setminus \Gamma_N$.

As can be seen from the above two examples, the Stokes iteration scheme has better stability, so we compute the solutions using the Stokes scheme. Setting $\nu = 0.1$, $\tau = h = 1/64$, we simulate the numerical solutions for the velocity and flux at $t = 1\,\text{s}$, $3\,\text{s}$, $5\,\text{s}$, $10\,\text{s}$, as shown in Figs. 3–6. Moreover, we compare the results obtained by the Stokes scheme with those obtained by the Newton and Oseen schemes at $t = 10\,\text{s}$ in Figs. 6–8. From these figures, we find that the numerical results of the Stokes scheme are presented with least oscillations. Hence, this also shows that the Stokes
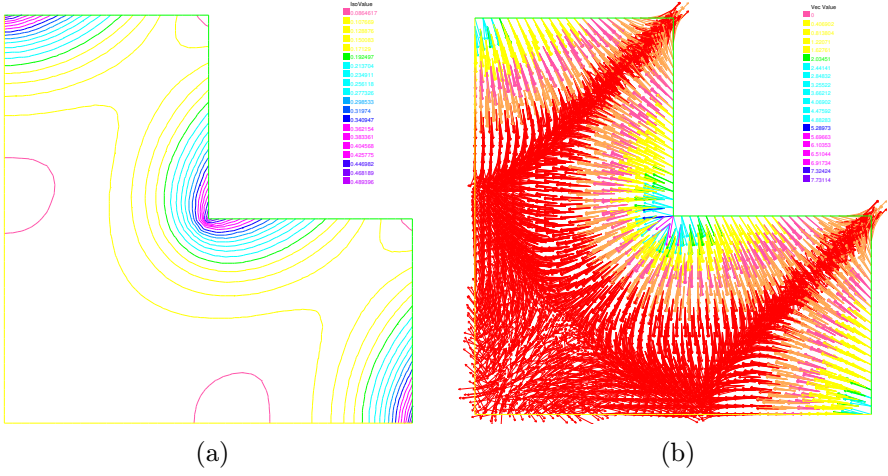
(a)   (b)

Figure 3. Stokes scheme for $\nu = 0.1$ and $t = 1$: (a) numerical solution of the velocity, (b) numerical solution of the flux.
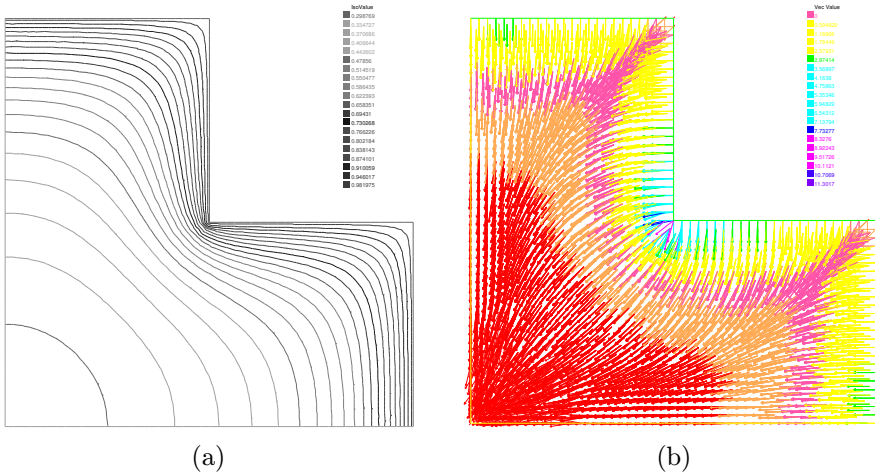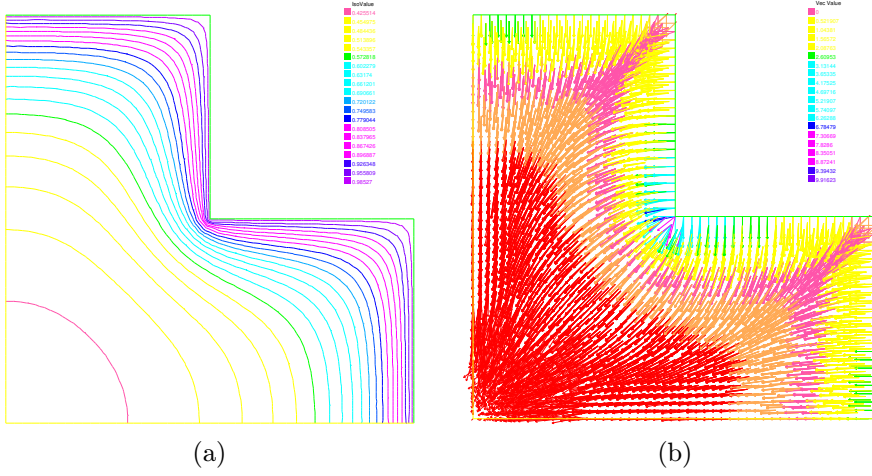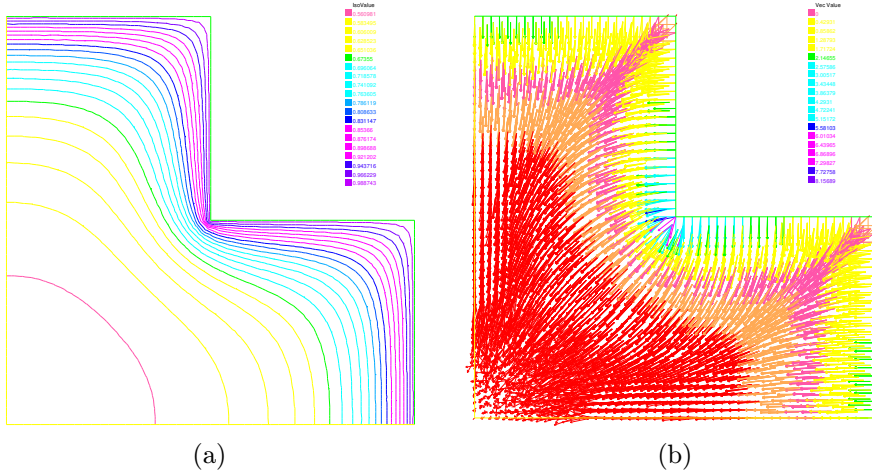

(a)   (b)

Figure 4. Stokes scheme for $\nu = 0.1$ and $t = 3$: (a) numerical solution of the velocity, (b) numerical solution of the flux.

scheme has better stability than the other two schemes. In fact, the time of the true solution tends to be large, the velocity and flux tend to the constants, i.e., due to

$$\lim_{t \to \infty} \exp\left(\frac{x + y - t}{2\nu}\right) = 0,$$

we have

$$\lim_{t \to \infty} u(x, y, t) = 1, \quad \lim_{t \to \infty} p(x, y, t) = (0, 0).$$

41

Figure 5. Stokes scheme for $\nu = 0.1$ and $t = 5$: (a) numerical solution of the velocity, (b) numerical solution of the flux.
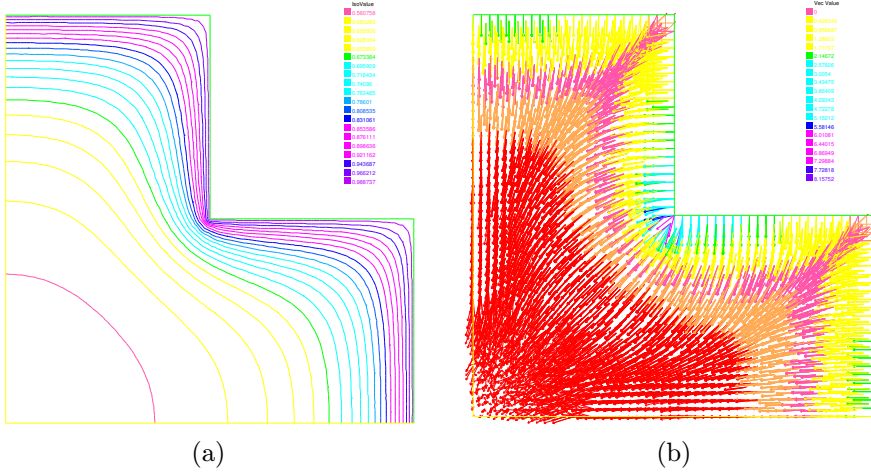

Figure 6. Stokes scheme for $\nu = 0.1$ and $t = 10$: (a) numerical solution of the velocity, (b) numerical solution of the flux.

So when the time tends to a certain value, the velocity and flux tends to the steady state. In fact, the velocity and flux of the final state are similar to Figs. 6–8.

6. CONCLUSIONS

In this paper, a new fully discrete mixed finite element method approximating the velocity and flux of Burgers' equation has been described. The spatial discretization is based on the lowest-order interpolations for the velocity and the flux; the time

(a)   (b)

Figure 7. Newton scheme for $\nu = 0.1$ and $t = 10$: (a) numerical solution of the velocity, (b) numerical solution of the flux.
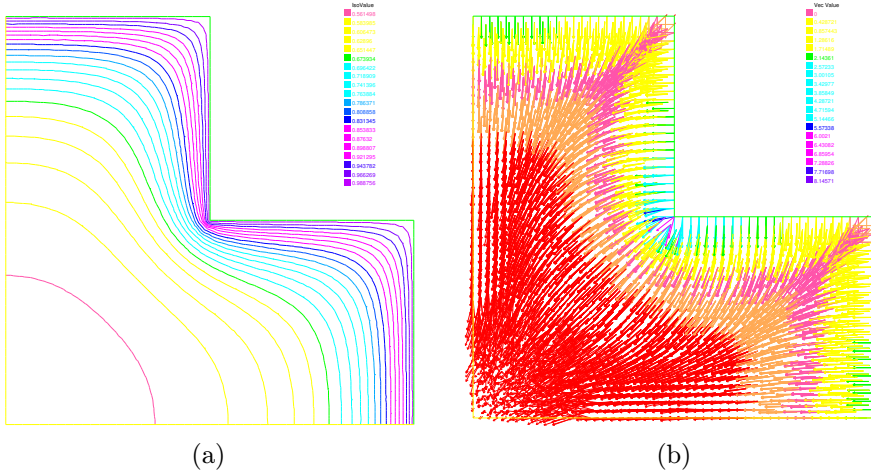

(a)   (b)

Figure 8. Oseen scheme for $\nu = 0.1$ and $t = 10$: (a) numerical solution of the velocity, (b) numerical solution of the flux.

discretization is based on the Crank-Nicolson scheme; and the nonlinear term is based on the Stokes scheme. A priori error estimate has been derived and the numerical experiment shows the efficiency of the given method. This method can be expanded to the case of three dimensions and other nonlinear problems.

References

[1] *R. A. Adams*: Sobolev Spaces. Pure and Applied Mathematics 65, Academic Press, New York, 1975. zbl MR

[2] *H. Bateman*: Some recent researches on motion of fluids. Mon. Weather Rev. *43* (1915), 163–170.

[3] *N. Bressan, A. Quarteroni*: An implicit/explicit spectral method for Burgers' equation. Calcolo *23* (1986), 265–284. zbl MR

[4] *J. Cadwell, P. Wanless, A. E. Cook*: A finite element approach to Burgers' equation. Appl. Math. Modelling *5* (1981), 189–193. zbl MR

[5] *H. Chen, Z. Jiang*: A characteristics-mixed finite element method for Burgers' equation. J. Appl. Math. Comput. *15* (2004), 29–51. zbl MR

[6] *P. G. Ciarlet*: The Finite Element Method for Elliptic Problems. Studies in Mathematics and Its Applications. Vol. 4, North-Holland Publishing Company, Amsterdam, 1978. zbl MR

[7] *J. Crank, P. Nicolson*: A practical method for numerical evaluation of solutions of partial differential equations of the heat-conduction type. Proc. Camb. Philos. Soc. *43* (1947), 50–67; Reprint in Adv. Comput. Math. *6* (1996), 207–226. zbl zbl MR M

[8] *Y. Duan, R. Liu*: Lattice Boltzmann model for two-dimensional unsteady Burgers' equation. J. Comput. Appl. Math. *206* (2007), 432–439. zbl MR

[9] *C. A. J. Fletcher*: A comparison of finite element and finite difference solutions of the one- and two-dimensional Burgers' equations. J. Comput. Phys. *51* (1983), 159–188. zbl MR

[10] *Y. He*: Two-level method based on finite element and Crank-Nicolson extrapolation for the time-dependent Navier-Stokes equations. SIAM J. Numer. Anal. *41* (2003), 1263–1285. zbl MR

[11] *Y. He, J. Li*: Convergence of three iterative methods based on the finite element discretization for the stationary Navier-Stokes equations. Comput. Methods Appl. Mech. Eng. *198* (2009), 1351–1359. zbl MR

[12] *Y. He, W. Sun*: Stability and convergence of the Crank-Nicolson/Adams-Bashforth scheme for the time-dependent Navier-Stokes equations. SIAM J. Numer. Anal. *45* (2007), 837–869. zbl MR

[13] *Y. He, W. Sun*: Stabilized finite element method based on the Crank-Nicolson extrapolation scheme for the time-dependent Navier-Stokes equations. Math. Comput. *76* (2007), 115–136. zbl MR

[14] *F. Hecht, O. Pironneau, A. Le Hyaric, K. Ohtsuka*: FREEFEM++, version 2.3-3, 2008. Software available at http://www.freefem.org.

[15] *J. G. Heywood, R. Rannacher*: Finite-element approximation of the nonstationary Navier-Stokes problem. IV. Error analysis for second-order time discretization. SIAM J. Numer. Anal. *27* (1990), 353–384. zbl MR

[16] *P. Huang, A. Abduwali*: The modified local Crank-Nicolson method for one- and two-dimensional Burgers' equations. Comput. Math. Appl. *59* (2010), 2452–2463. zbl MR

[17] *H. Johnston, J. G. Liu*: Accurate, stable and efficient Navier-Stokes solvers based on explicit treatment of the pressure term. J. Comput. Phys. *199* (2004), 221–259. zbl MR

[18] *Z. Luo, R. Liu*: Mixed finite element analysis and numerical simulation for Burgers equation. Math. Numer. Sin. *21* (1999), 257–268. (In Chinese.) zbl MR

[19] *A. K. Pany, N. Nataraj, S. Singh*: A new mixed finite element method for Burgers' equation. J. Appl. Math. Comput. *23* (2007), 43–55. zbl MR

[20] *Y. Shang*: Initial-boundary value problems for a class of generalized KdV-Burgers equations. Math. Appl. *9* (1996), 166–171. (In Chinese.) zbl MR

[21] *L. Shao, X. Feng, Y. He*: The local discontinuous Galerkin finite element method for Burger's equation. Math. Comput. Modelling *54* (2011), 2943–2954. zbl MR

44

[22] *F. Shi, J. Yu, K. Li*: A new stabilized mixed finite-element method for Poisson equation based on two local Gauss integrations for linear element pair. Int. J. Comput. Math. *88* (2011), 2293–2305. zbl MR

[23] *Z. Weng, X. Feng, P. Huang*: A new mixed finite element method based on the Crank-Nicolson scheme for the parabolic problems. Appl. Math. Modelling *36* (2012), 5068–5079. zbl MR

Authors' address: *Xiaohui Hu, Pengzhan Huang* (corresponding author), *Xinlong Feng*, College of Mathematics and System Sciences, Xinjiang University, Urumqi 830046, P. R. China, e-mail: 1711175247@qq.com, hpzh007@yahoo.com, fxlmath@xju.edu.cn.